

Unusual crystallization behavior close to the glass transition.

Caroline Desgranges, and Jerome Delhommelle

Department of Chemistry, University of North Dakota, Grand Forks ND 58202

(Dated: April 13, 2021)

Abstract

Using molecular simulations, we shed light on the mechanism underlying crystal nucleation in metal alloys and unravel the interplay between crystal nucleation and glass transition, as the conditions of crystallization lie close to this transition. While decreasing the temperature of crystallization usually results in a lower free energy barrier, we find an unexpected reversal of behavior for glass-forming alloys as the temperature of crystallization approaches the glass transition. For this purpose, we simulate the crystallization process in two glass-forming Copper alloys, Ag_6Cu_4 , which has a positive heat of mixing, and in $CuZr$, characterized by a large negative heat of mixing. Our results allow us to identify that this unusual behavior is directly correlated with a non-monotonic temperature dependence for the formation energy of connected icosahedral structures, which are incompatible with crystalline order and impede the development of the crystal nucleus, leading to an unexpectedly larger free energy barrier at low temperature. This, in turn, promotes the formation of a predominantly closed-packed critical nucleus, with fewer defects, thereby suggesting a new way to control the structure of the crystal nucleus, which is of key importance in catalysis.

The formation of crystalline and amorphous solids are key processes in solid-state physics and chemistry^{1,2}, with applications in pharmaceuticals, electronics and nanoscience. Crystals have properties that strongly depend on their structure, and can be tailored by modifying the conditions of crystallization². Amorphous solids or glasses can be extremely advantageous as their properties can outperform those of their crystalline counterparts, as e.g. amorphous solids of pharmaceutical compounds are often more soluble in water and metallic glasses exhibit improved magnetic and mechanical properties^{3,4}. It is therefore crucial to understand how the competition between crystallization and glass formation takes place at the microscopic level to be able to control the type of material obtained.

The microscopic structure of supercooled liquids has become increasingly pictured as inhomogeneous^{3,5-7}. It results from the existence, within the supercooled liquid of short-range order structures, e.g. icosahedral short-range order (ISRO) as discussed in Frank's pioneering work⁸, and of medium-range order (MRO), which are larger domains, either crystal-like⁹ or composed of connected icosahedra¹⁰. The subtle balance between the two types of order has a complex, yet fascinating, impact on crystallization. On the one hand, icosahedral structures are structurally incompatible with crystalline order and lead to an enhancement of the glass-forming ability⁵. On the other hand, amorphous precursors have been shown to promote crystallization during biomineralization¹¹ and fast crystal growth modes have been reported in glasses¹²⁻¹⁵. In this work, we focus on the crystal nucleation process, and show that the free energy of nucleation in a metallic glass-forming liquid exhibits a non-monotonic temperature dependence, contrary to the expected behavior². To analyze this, we determine the formation energy of connected ISROs¹⁶, and show that the formation energy of connected ISROs with a large node degree also exhibits a non-monotonic temperature dependence. This correlation between two non-monotonic behaviors sheds new light on the competition between the onset of crystalline order and the formation of connected icosahedra that takes place in a supercooled liquid.

Metallic glasses have recently been used to prepare nanoscale catalytic fibers⁴. Similarly, metal nanocrystals have applications in a wide array of fields, e.g. in biology¹⁷ and chemistry¹⁸. In bimetallic alloys, a competition between glass transition and crystallization can be triggered by the choice of the metals involved. The relative sizes of the two metals plays a major role in the formation of glasses, with very dissimilar radii for the two metals (with a ratio of 1.1 and above) favoring the onset of a glass transition. Here, we focus on the Ag_6Cu_4

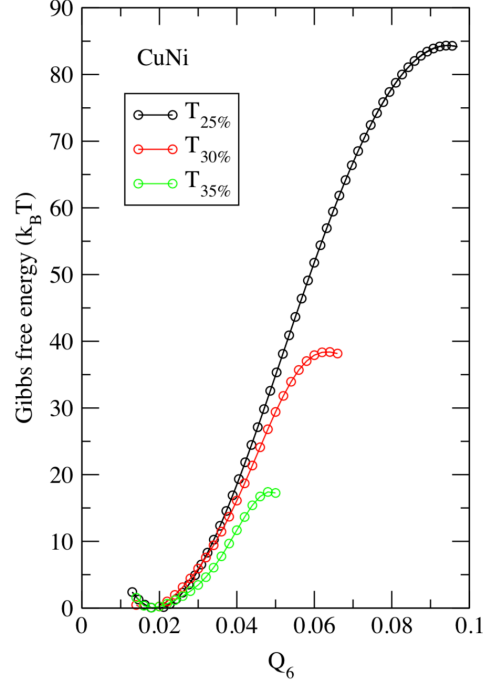
and $CuZr$ alloys. Both exhibit a large size ratio ($r_{Ag} : r_{Cu} = 1.13$ and $r_{Zr} : r_{Cu} = 1.244$) and become a glass below 500 K for Ag_6Cu_4 and 700 K for $CuZr$ ^{19,20}. To examine the interplay between crystallization and glass transition, we study crystal nucleation from increasingly supercooled liquids, i.e. closer and closer to the glass transition. To identify the effect of the glass transition on nucleation, we also examine the impact of supercooling on $CuNi$, for which the size difference is less than 2.5% and no glass transition is observed.

We model the interactions between metal atoms using embedded atom model potentials^{19,20}, that have been shown to model accurately metal properties, with e.g. a predicted melting temperature of 1090 K for Ag_6Cu_4 , in excellent agreement with experiments (1053 K) and a glass transition around 500 K¹⁹. We simulate crystal nucleation for increasing degrees of supercooling for Ag_6Cu_4 , $CuZr$ and $CuNi$. The formation of a crystal nucleus of a critical size is an activated process associated with a large free energy barrier, due to the cost of creating a crystal nucleus within a liquid. To determine this free energy barrier, we combine molecular dynamics simulations with an umbrella sampling (US) approach^{21,22}, and the Q_6 order parameter that captures the onset of crystalline order^{23–25}. This method allows²⁴ us to stabilize the system at each step of the nucleation process, enabling the collection of average properties over long simulation runs. The nucleation pathway is typically split into 15 US windows, for which the US potential maintains the system around a fixed value for the order parameter Q_6 . For each simulation window, we perform a first simulation run to reach the target value for Q_6 and to allow the system to relax. Then, once the system has reached a steady-state, we carry out a second production run over which averages are collected²⁵. We perform simulations under isothermal and isobaric conditions ($P = 1$ atm). The temperatures of crystallization range from 708.5 K to 599.5 K for Ag_6Cu_4 (i.e. for degrees of supercooling from 35% to 45%), from 840 K to 728 K for $CuZr$ (i.e. for degrees of supercooling from 40% to 48%) and from 1132.5 K to 981.5 K for $CuNi$ (or degrees of supercooling from 25% to 35%). The free energy barrier of nucleation, as well as the size and structure of the critical nuclei are determined from the US simulations, as discussed in prior work^{24,25}. The size and structure of the critical nucleus are determined using the criteria defined by Frenkel *et al.*^{21,22,25,26} during the course of the US simulation window when the system is at the top of the free energy barrier. Specifically, an atom is identified as having a solid-like environment if more than 6 of their nearest neighbors show a highly correlated local environment (i.e. with a dot product of their q_{6l} vectors greater than 0.6)²⁷.

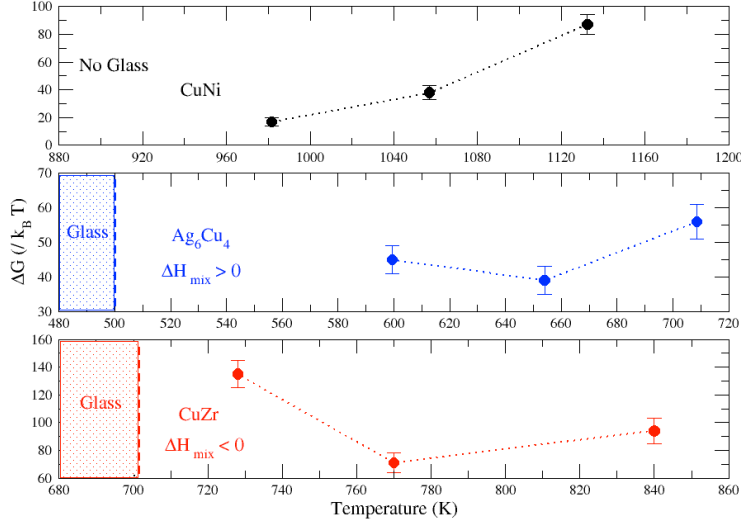
The size of the nucleus is then determined through a cluster analysis. We add that the critical nuclei generated during the *US* simulations have been checked to be genuine critical nuclei in unbiased simulations²².

We first discuss the results obtained for the free energy of nucleation for *CuNi*. Fig. 1(a) shows the free energy profile of nucleation for degrees of supercooling ranging from 25% to 35%. For each temperature, we gradually increase the imposed value for Q_6 and observe, as a result, the formation of a crystal nucleus. When the system reaches the top of the free energy barrier, we obtain a critical nucleus that can either continue to grow, or dissolve back into the liquid. As shown in Fig. 1(a), increasing the degree of supercooling results in the following trend. We observe that the height of the free energy barrier is higher for a low supercooling, with a free energy of nucleation estimated at $87 \pm 7 k_B T$ for $T_{25\%}$, at $38 \pm 5 k_B T$ for $T_{30\%}$, and at $17 \pm 3 k_B T$ for $T_{35\%}$. Furthermore, the monotonic variation, found for the nucleation free energy with the degree of supercooling, is in line with the predictions from the classical nucleation theory² and with prior simulation results on binary ionic systems²⁸ and pure metals²⁹. Turning to the results obtained for the two glass-forming copper alloys, we observe a dramatically different behavior in Fig. 1(b). Unlike for *CuNi*, we find that the free energy of nucleation exhibit non-monotonic variations with the degree of supercooling. For *Ag₆Cu₄*, the free energy of nucleation starts by decreasing from $56 \pm 5 k_B T$ ($T_{35\%}$) to $39 \pm 4 k_B T$ ($T_{40\%}$), before increasing again to $45 \pm 4 k_B T$ for $T_{45\%}$. Similarly, Fig. 1(b) shows that, for the *CuZr* alloy, the free energy of nucleation also exhibits a non-monotonic dependence on temperature, as it first decreases from $94 \pm 9 k_B T$ ($T_{40\%}$) to $71 \pm 7 k_B T$ ($T_{45\%}$), before increasing again to $135 \pm 10 k_B T$ for $T_{48\%}$. This behavior strongly departs from the predictions of the classical nucleation theory, and from the results for the non-glass forming *CuNi*. This shows that, as the conditions of crystallization for *Ag₆Cu₄* and *CuZr* get closer to the glass transition, we observe an unusual, non-monotonic, crystallization behavior.

To analyze this, we examine the effect of supercooling on the parent phase and show in Fig. 2 the pair distribution functions ($G(r)$) in the metastable liquid for *Ag₆Cu₄* in the absence of any *US* potential. $G(r)$ displays, as T decreases, the expected increase in the height of the first peak, characteristic of the increase in SRO, coupled with a decrease in the minimum that immediately follows. These functions also reveal a subtle change in $G(r)$, with a splitting of the second peak at low temperature. The same behavior has also been reported²⁰ in the case of *CuZr*. This indicates that the system approaches the



(a)



(b)

FIG. 1: (a) Gibbs free energy profiles of nucleation for liquid *CuNi* for different degrees of supercooling, and (b) ΔG as a function of temperature for *CuNi* and for the two glass-forming Copper alloys *Ag₆Cu₄* and *CuZr*.

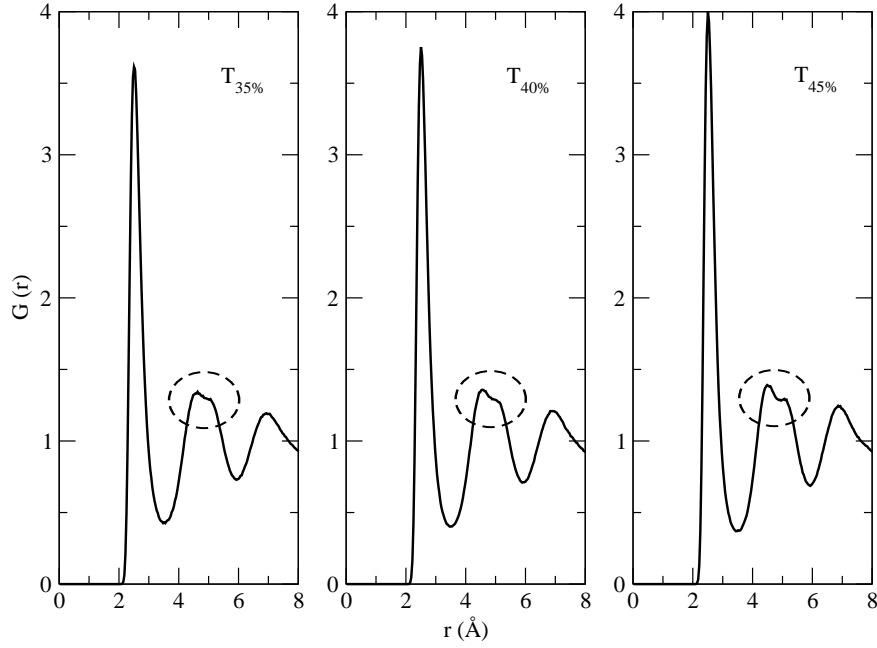


FIG. 2: Copper-Copper pair distribution function $G(r)$ in supercooled Ag_6Cu_4 liquids for a supercooling of 35% (left), 40% (middle) and 45% (right). The circled regions show the splitting of the second maximum in $G(r)$.

glass transition¹⁹, and points to the development of MRO in the liquid³⁰. This stems from the increased geometric frustration⁵, as non space-filling clusters, such as e.g. icosahedral short-range order (ISRO), form in the supercooled liquid and prevent the onset of crystal nucleation. Recent experiments on metallic glasses⁷ have provided support for an icosahedral order-based frustration model in such systems. Furthermore, the increase in icosahedral order has been linked to the splitting of the second peak of $G(r)$ ³⁰. We therefore start by quantifying the ISROs²⁹. Following the analysis of Wu *et al.*¹⁶, we find that the presence of ISROs goes on to impact the MRO in the supercooled liquid, with the increase, as temperature decreases, of connections between ISROs via volume sharing (see Fig. 3(a)). Upon closer inspection, Fig. 3(a) shows that a decrease from $T_{40\%}$ to $T_{45\%}$ results in a much more significant increase in the number density of larger clusters of connected ISROs, than the decrease from $T_{35\%}$ to $T_{40\%}$. To understand this, we calculate in Fig. 3(b) the ISRO

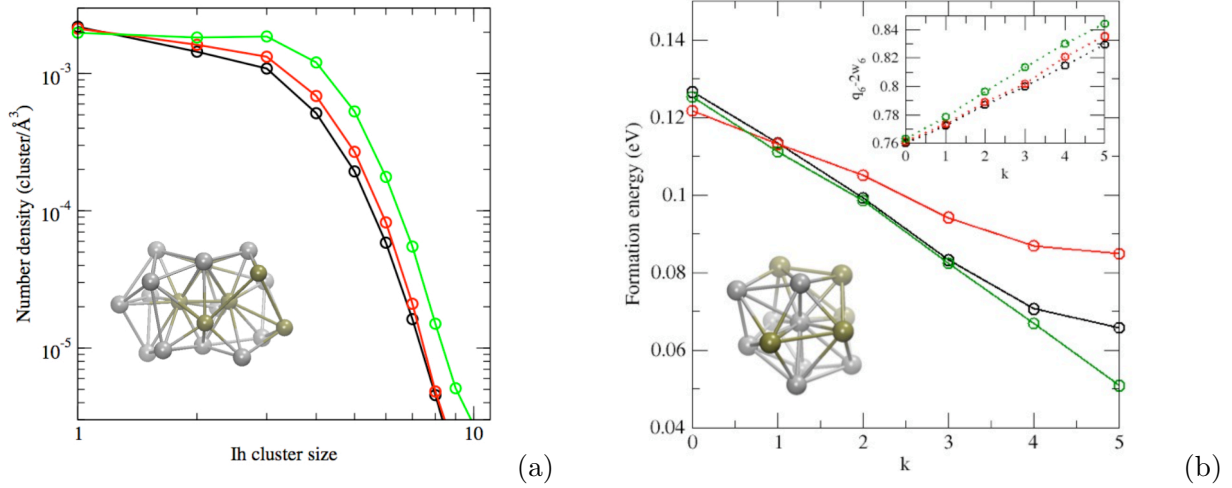


FIG. 3: Supercooled Ag_6Cu_4 . (a) Number density distributions of clusters formed by connected ISROs via volume sharing at $T_{35\%}$ (black), $T_{40\%}$ (red) and $T_{45\%}$ (green), with a snapshot showing 2 connected ISROs. (b) ISRO formation energy as a function of the node degree k , with a snapshot showing a configuration for $k = 0$. The inset shows the increase in the Ih order parameter with k .

formation energy as a function of the node degree k , i.e. the number of ISROs directly connected to it. In this calculation, we set the reference for the energy of each atom to its value in the *FCC* crystal for *Ag* and *Cu*, as in previous work¹⁶. This plot shows a decrease in the formation energy as k increases, in line with prior work on supercooled *CuZr*. Turning to the temperature dependence of the results, we find that the formation energy for larger k values increases when T decreases from $T_{35\%}$ to $T_{40\%}$. Since fewer connected ISROs are expected to favor crystallization, this greater formation energy for connected ISROs at $T_{40\%}$ is consistent with the decrease in the free energy of nucleation found in Fig. 1(b). On the other hand, the formation energy for the larger k undergoes a significant decrease with T going from $T_{40\%}$ to $T_{45\%}$. This means that multiple connections between ISROs form much more easily at $T_{45\%}$. Since connected ISROs lead to a MRO incompatible with crystalline order, the much lower formation energy for $T_{45\%}$ is also consistent with the increase in the free energy of nucleation at this temperature. These results therefore establish a direct correlation between the non-monotonic temperature dependence of the free energy of nucleation and the non-monotonic temperature dependence of the formation energy of connected ISROs for $k > 2$.

How does this impact the nucleation process? As shown in Fig. 4, the crystal nucleus is

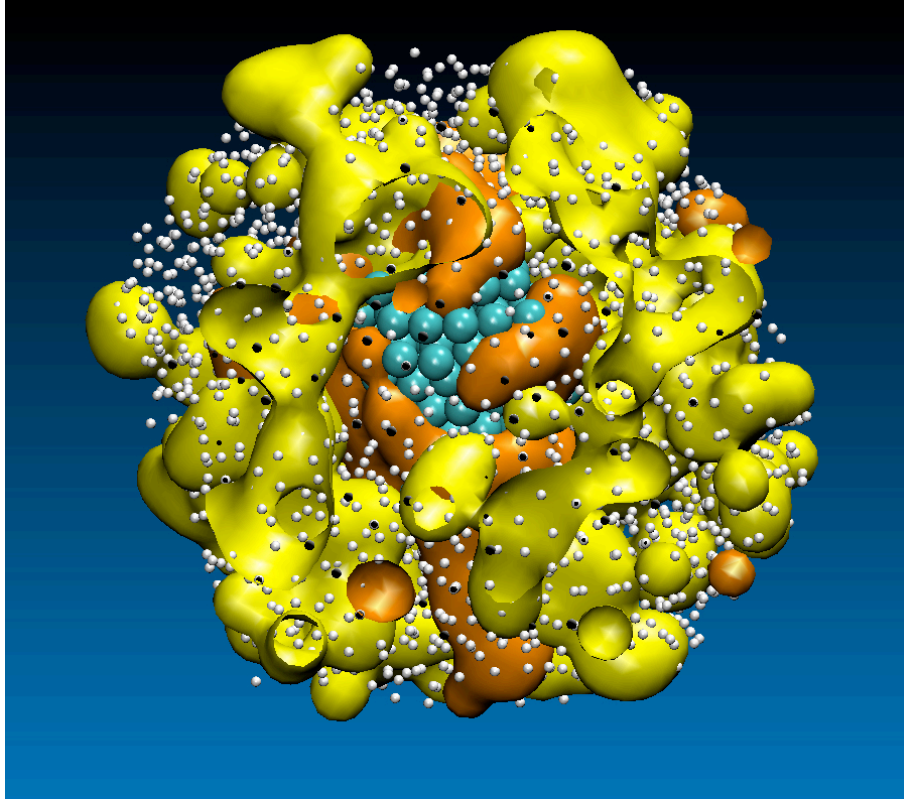


FIG. 4: Formation of the critical nucleus for the Ag_6Cu_4 system ($T_{45\%}$). The crystal nucleus (cyan) is surrounded by a crystal-like ordered region (orange), by ISROs (yellow) and liquid-like atoms (white).

surrounded by a supercooled liquid that exhibits two different types of order. These correspond to the connected ISROs and to a crystal-like region, characterized by large Steinhardt order parameters⁹, around the crystal nucleus⁵. The presence of connected ISROs hinders the nucleation process, and results in a larger free energy barrier for the nucleation process. We add that the density of ISROs around the crystal nucleus is the same as in the bulk, and that no enrichment in ISROs occurs during crystal nucleation. Finally, we find much lower number densities of ISROs for $CuNi$, which ultimately result in the usual monotonic temperature dependence for the nucleation free energy in the non glass-former $CuNi$.

We now turn to the size and structure of the critical nucleus in Fig. 5 and focus for comparison purposes on the two alloys, $CuNi$ and Ag_6Cu_4 , for which both elements form FCC crystals. For $CuNi$, the critical size decreases steadily from 517 ± 40 atoms ($T_{25\%}$) to 74 ± 15 atoms ($T_{35\%}$). This monotonic behavior is in line with the predictions from the

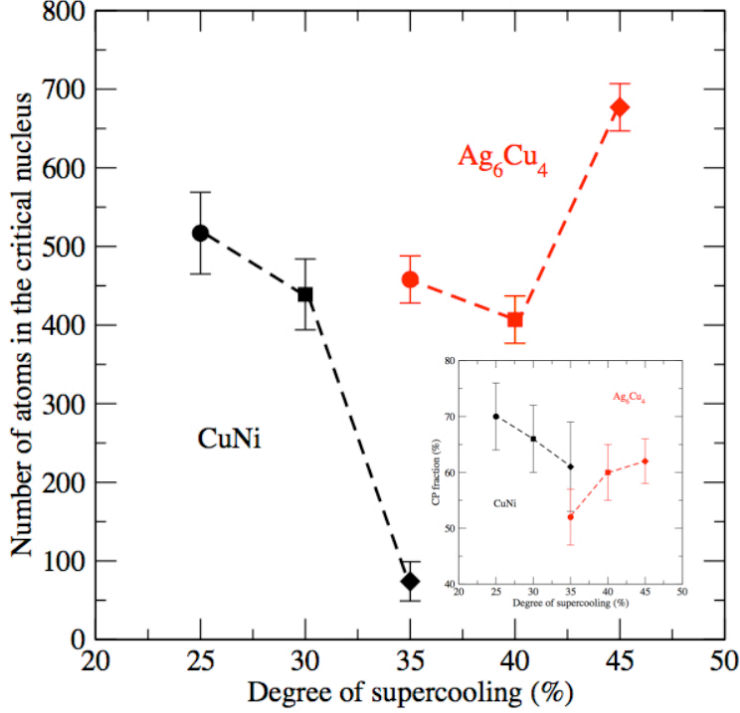


FIG. 5: Variation of the size of the critical nucleus as a function of the degree of supercooling. (Inset) Structure of the critical nucleus against the degree of supercooling.

classical nucleation theory. Fig. 5 also shows that the fraction in the stable close-packed (*CP*) structure decreases as the degree of supercooling increases, since all polymorphs form easily at low temperature. For Ag_6Cu_4 , we observe very different behaviors. First, the critical size decreases from 458 ± 30 atoms ($T_{35\%}$) to 407 ± 25 atoms ($T_{40\%}$) and then increases back to 677 ± 40 ($T_{45\%}$). This non-monotonic behavior is consistent with the variations observed for the nucleation free energy. Second, the structure becomes more dominated by the stable *CP* structure as the degree of supercooling increases. This is likely a consequence of the role played by the ISROs surrounding the crystal nucleus, which slow down nucleation and lead to a nucleus with fewer defects. This increase in *CP* fraction correlates well with the increase in the density of ISROs in the supercooled liquid, thereby providing support for this mechanism. It also suggests a new way of controlling polymorphism by setting the conditions of crystallization close to the glass transition.

Our results show that an unexpected crystallization behavior arises, as the system approaches the glass transition. Close to this transition, a further decrease in temperature

results in a reversal of crystallization behavior, with the formation of a larger critical nucleus associated with a larger free energy barrier of nucleation. This unusual behavior is directly correlated with a non-monotonic temperature dependence for the formation energy of connected icosahedral structures. Given the existence of a glass transition for molecular and pharmaceutical compounds¹⁴, the conclusions drawn here extend to a wide range of systems, well beyond the case of metallic systems.

Acknowledgements Partial funding for this research was provided by the National Science Foundation (NSF) through CAREER award DMR-1052808.

-
- ¹ P. G. Debenedetti and F. H. Stillinger, *Nature* **410**, 259 (2001).
 - ² J. Bernstein, *Polymorphism in molecular crystals* (Clarendon Press, Oxford, 2002).
 - ³ A. Hirata, L. Kang, T. Fujita, B. Klumov, K. Matsue, M. Kotani, A. Yavari, and M. Chen, *Science* **341**, 376 (2013).
 - ⁴ J. Schroers, *Physics Today* **66**, 32 (2013).
 - ⁵ H. Tanaka, *Eur. Phys. J. E* **35**, 113 (2012).
 - ⁶ A. Hirata, P. Guan, T. Fujita, Y. Hirotsu, A. Inoue, A. R. Yavari, T. Sakurai, and M. Chen, *Nat. Mater.* **10**, 28 (2011).
 - ⁷ Y. Shen, T. Kim, A. Gangopadhyay, and K. Kelton, *Phys. Rev. Lett.* **102**, 057801 (2009).
 - ⁸ F. Frank, *Proc. R. Soc. A* pp. 43–46 (1952).
 - ⁹ M. Leocmach and H. Tanaka, *Nat. Commun.* **3**, 974 (2012).
 - ¹⁰ H. Sheng, W. Luo, F. Alamgir, J. Bai, and E. Ma, *Nature* **439**, 419 (2006).
 - ¹¹ S. Weiner, I. Sagi, and L. Addadi, *Science* **309**, 1027 (2005).
 - ¹² T. Hikima, Y. Adachi, M. Hanaya, and M. Oguni, *Phys. Rev. B* **52**, 3900 (1995).
 - ¹³ T. Konishi and H. Tanaka, *Phys. Rev. B* **76**, 220201 (2007).
 - ¹⁴ Y. Sun, H. Xi, S. Chen, M. Ediger, and L. Yu, *J. Phys. Chem. B* **112**, 5594 (2008).
 - ¹⁵ J. Orava and A. L. Greer, *J. Chem. Phys.* **140**, 214504 (2014).
 - ¹⁶ Z. Wu, F. Li, C. Huo, M. Li, W. Wang, and K. Liu, *Sci. Rep.* **6** (2016).
 - ¹⁷ M. R. Langille, J. Zhang, M. L. Personick, S. Li, and C. A. Mirkin, *Science* **337**, 954 (2012).

- ¹⁸ H. Zheng, R. K. Smith, Y.-w. Jun, C. Kisielowski, U. Dahmen, and A. P. Alivisatos, *Science* **324**, 1309 (2009).
- ¹⁹ Y. Kimura, Y. Qi, T. Cagin, and W. A. Goddard, *Phys. Rev. B* **59**, 3527 (1999).
- ²⁰ G. Duan, D. Xu, Q. Zhang, G. Zhang, T. Cagin, W. L. Johnson, and W. A. Goddard III, *Phys. Rev. B* **71**, 224208 (2005).
- ²¹ P. R. ten Wolde, M. J. Ruiz-Montero, and D. Frenkel, *Phys. Rev. Lett.* **75**, 2714 (1995).
- ²² C. Desgranges and J. Delhommelle, *Phys. Rev. Lett.* **98**, 235502 (2007).
- ²³ U. Gasser, E. R. Weeks, A. Schofield, P. N. Pusey, and D. A. Weitz, *Science* **292**, 258 (2001).
- ²⁴ S. Auer and D. Frenkel, *Nature* **409**, 1020 (2001).
- ²⁵ C. Desgranges and J. Delhommelle, *J. Am. Chem. Soc.* **136**, 8145 (2014).
- ²⁶ S. Auer and D. Frenkel, *Nature* **409**, 1023 (2001).
- ²⁷ C. Desgranges and J. Delhommelle, *J. Phys. Chem. C* **120**, 27657 (2016).
- ²⁸ C. Valeriani, E. Sanz, and D. Frenkel, *J. Chem. Phys.* **122**, 194501 (2005).
- ²⁹ C. Desgranges and J. Delhommelle, *J. Chem. Phys.* **127**, 144509 (2007).
- ³⁰ Y.-C. Liang, R.-S. Liu, Y.-F. Mo, H.-R. Liu, Z.-A. Tian, Q.-y. Zhou, H.-T. Zhang, L.-L. Zhou, Z.-Y. Hou, and P. Peng, *J. Alloy. Comp.* **597**, 269 (2014).